



Seismic analysis of a full scaled self-supported tower using ambient vibration testing

Ahmed M. A. Sayed¹ · Ahmed H. Yousef¹ · Ghada N. Saudi² · Ehab H. A. Hassan²

Received: 16 March 2022 / Accepted: 8 November 2022 / Published online: 20 November 2022
© Springer Nature Switzerland AG 2022

Abstract

This paper presents the structural investigation of a 50 m existing self-supported tower located in Ismailia, Egypt. The investigation was carried out using experimental ambient vibration test (AVT) and seismic structural analysis. The study is to be considered one of the few studies for the dynamic testing of full scale self-supporting towers using AVT techniques. The dynamic properties were identified for the full scale self-supported tower using a set of eighteen uniaxial accelerometers installed in different positions and altitudes over the tower, roving of accelerometers took place during field measurements. The experimental modal results were identified in terms of its natural frequencies and mode shapes. The Enhanced Frequency Domain Decomposition (EFDD) and Stochastic Subspace Identification–Canonical Variate Analysis (SSI-CVA) methods were applied to extract the modal properties of the tower. The results obtained showed good agreement between both methods. The modal behavior was investigated in the range between 0 and 20.5 Hz. Finite element model was updated based on the identified dynamic properties. Finally, the structural analysis under seismic loads was also studied using time history analysis. The results illustrate the success of AVT in identifying the actual dynamic properties of the full scale self-supporting tower, where a finite element model was reliably updated to represent the actual dynamic behavior of the tower. The seismic structural analysis was enhanced using the updated model as the structural results expresses the real structural status of the existing tower using both the experimental and the analytical techniques.

Keywords Self-supported tower · Full scale testing · Natural frequency · Dynamic behavior · Ambient vibration testing · Modal analysis · Finite element model · Seismic analysis

Introduction

Nowadays, almost every communication method is wireless. Telecommunication towers form one of the most essential components of any telecom network, thus it is not only used by cell phone providers for phone calls and internet but also used by police and ambulance to obtain their wireless communications and provide a quality service. Studies have been carried over the years to study the effect of different dynamic loads such as wind, ice loading and seismic loadings. Although, it was clear that only few studies carried out the experimental investigations either from existing structures

or applied to scale models in wind tunnels or shaking tables [1–3]. Also, it was found that vibration measurements to full scale structures would lead to enhancing the accuracy of finite element model through calibration with its measured properties. That technique has been applied into large civil structures such as bridges [4–7], dams, high rise buildings [8], towers [1–3, 9–14], and monuments [15–17]. In context of ongoing consulting project for assessment of telecommunication towers across Egypt, the project is implied in structures and metallic constructions research institute, Housing and Building National Research Center (HBRC); the 50 m height self-supporting tower was selected to perform a full structural seismic study using AVT techniques and FE model analysis. In this paper, the identification of natural frequencies and their corresponding mode shapes through measuring the ambient response of a full scale self-support tower was performed. The ambient vibration testing (AVT) is considered an output-only response technique for dynamic test method. Moreover, AVT test method has the

✉ Ahmed M. A. Sayed
ahmed_magdy_d@hotmail.com

¹ Ain Shams University, Cairo, Egypt

² Structures and Metallic Constructions Research Institute, HBRC, Cairo, Egypt

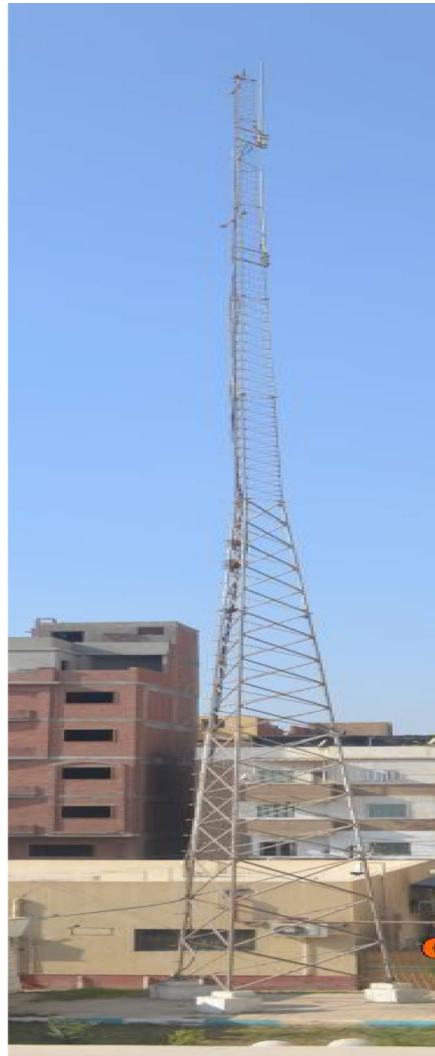
advantage of being a cost effective, because there is no need for the structure to be excited using special instruments. Therefore, AVT is considered as an effective non-destructive test and being harmless to the tested structure [18]

Structural parameters were used to produce the global modes interpreting the experimentally identified peaks in the spectral analysis. The modal behavior was investigated in the range 0–20.50 Hz. The first fundamental natural frequency of the self-support tower was identified at 0.5704 Hz. A verification based on the measurements has been carried using ANSYS and it shows good agreement between the experimental results and the finite element model. Furthermore, a study on the effect of seismic loads on the tower was conducted using 1995 Gulf of Aqaba earthquake time history records.

The self-supported tower

The tower was constructed back in 1985 in Ismalia, Egypt. The tower components are shown in Fig. 1. The geometrical properties were measured in the field using a vernier and a metal thickness detector. The tower is a 50 m steel tower is an equilateral triangle in plan of size 3.23 m and at top 0.28 m, as shown in Fig. 2. The lower part of the tower starting at the ground level consists of 3 main legs of steel hollow pipe cross sections with dimensions of diameter 76 mm and 5.5 mm thickness. These leg members are interconnected by bolted connections. Steel angles cross section with dimensions of $45 \times 45 \times 3.5$ mm thickness are used as bracing connecting the main legs. The tower is supported on a reinforced concrete foundation under each leg.

Fig. 1 The components of self-supported tower



The 50 m self-supported tower



The tower foundations



Tower base

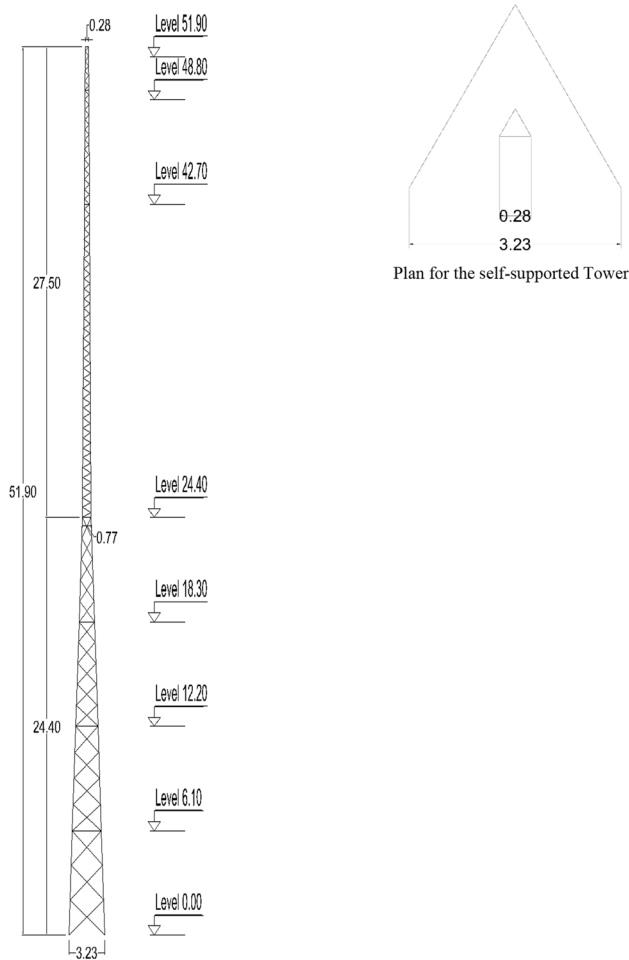


Fig. 2 Geometric Properties of the self-supported tower

Fig. 3 Direction of measurements at different levels

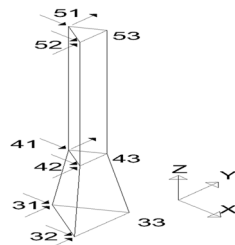


Table 1 Test grid details

| Setup No | Height (m) | Test Grid Point | Direction | Remarks | Setup |
|------------|------------|-----------------|-----------|-----------|---------|
| Chanel 1-1 | 48.80 | 61 | X | Reference | Setup 1 |
| Chanel 1-2 | 48.80 | 61 | Y | Reference | |
| Chanel 1-3 | 48.80 | 62 | X | Reference | |
| Chanel 1-4 | 48.80 | 62 | Y | Reference | |
| Chanel 1-5 | 48.80 | 63 | X | Reference | |
| Chanel 1-6 | 48.80 | 63 | Y | Reference | |
| Chanel 2-1 | 42.70 | 51 | X | Reference | Setup 2 |
| Chanel 2-2 | 42.70 | 51 | Y | Reference | |
| Chanel 2-3 | 42.70 | 52 | X | Reference | |
| Chanel 2-4 | 42.70 | 52 | Y | Reference | |
| Chanel 2-5 | 24.40 | 41 | X | – | |
| Chanel 2-6 | 24.40 | 41 | Y | – | |
| Chanel 3-1 | 24.40 | 42 | X | – | Setup 2 |
| Chanel 3-2 | 24.40 | 42 | Y | – | |
| Chanel 3-3 | 12.20 | 21 | X | – | |
| Chanel 3-4 | 12.20 | 21 | Y | – | |
| Chanel 3-5 | 12.20 | 22 | X | – | |
| Chanel 3-6 | 12.20 | 22 | Y | – | |
| Chanel 1-1 | 48.80 | 61 | X | Reference | Setup 2 |
| Chanel 1-2 | 48.80 | 61 | Y | Reference | |
| Chanel 1-3 | 48.80 | 62 | X | Reference | |
| Chanel 1-4 | 48.80 | 62 | Y | Reference | |
| Chanel 1-5 | 48.80 | 63 | X | Reference | |
| Chanel 1-6 | 48.80 | 63 | Y | Reference | |
| Chanel 2-1 | 42.70 | 51 | X | Reference | Setup 2 |
| Chanel 2-2 | 42.70 | 51 | Y | Reference | |
| Chanel 2-3 | 42.70 | 52 | X | Reference | |
| Chanel 2-4 | 42.70 | 52 | Y | Reference | |
| Chanel 2-5 | 18.30 | 31 | X | – | |
| Chanel 2-6 | 18.30 | 31 | Y | – | |
| Chanel 3-1 | 18.30 | 32 | X | – | Setup 2 |
| Chanel 3-2 | 18.30 | 32 | Y | – | |
| Chanel 3-3 | 6.10 | 11 | X | – | |
| Chanel 3-4 | 6.10 | 11 | Y | – | |
| Chanel 3-5 | 6.10 | 12 | X | – | |
| Chanel 3-6 | 6.10 | 12 | Y | – | |

Insitu ambient vibration test (AVT)

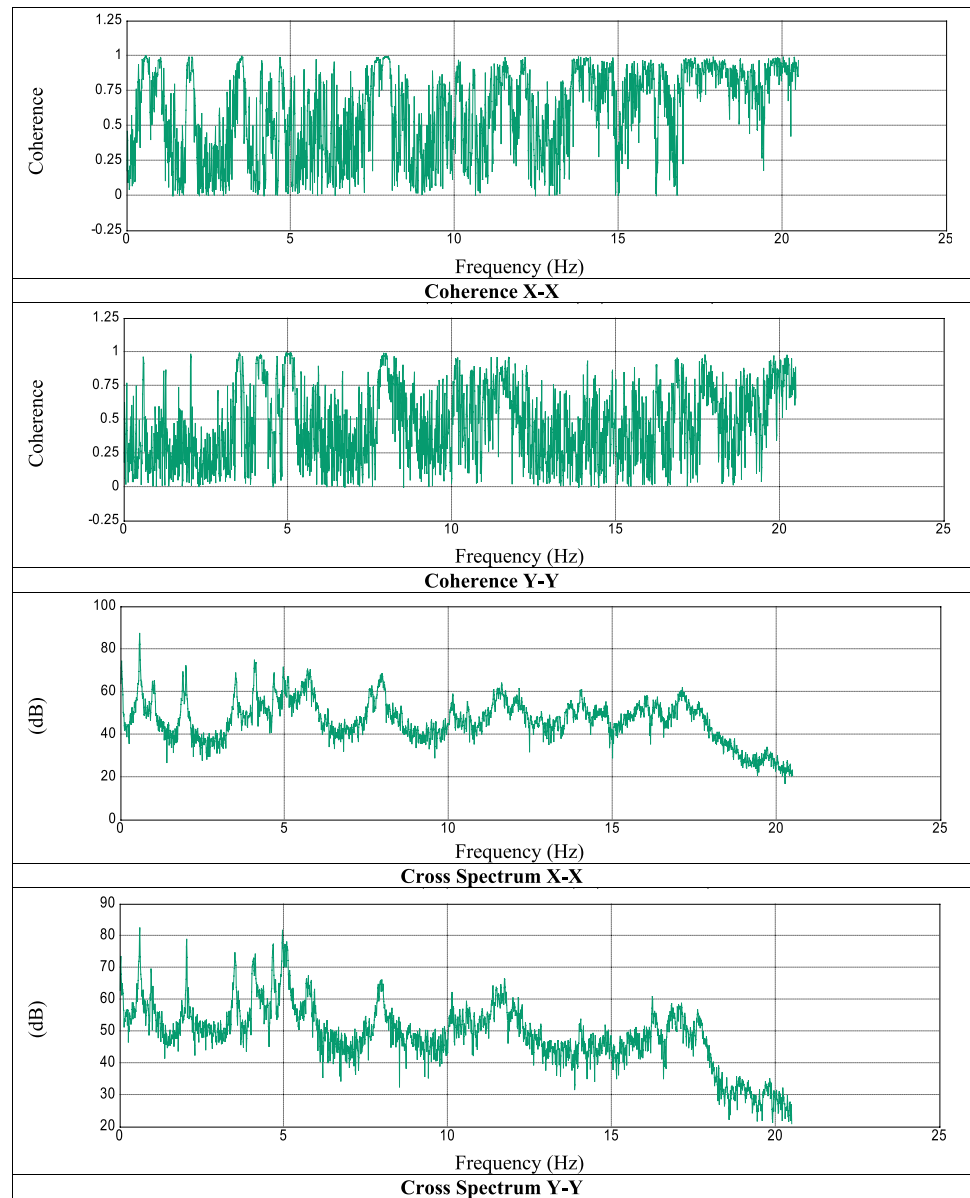
The ambient dynamic response was measured using the following:

- (a) Eighteen uniaxial piezoelectric accelerometers (PCB Model 393B04) of high sensitivity. The sensitivity of each accelerometer was determined using a calibrator exciter of type 4294 manufactured by Brüel & Kjær, the

sensitivity of each is 1000 mV/g, a measurement range of ± 5 g and frequency range 0.06 to 450 Hz.

- (b) PULSE analyzer type 3650/B manufactured by Brüel & Kjær.
- (c) PULSE LAN-XI analyzer with dynamic range of 160 dB manufactured by Brüel & Kjær, which has real-time capabilities for FFT analysis, order tracking and time data recording on multi channels.

Fig. 4 Results of signal processing



- (d) A notebook with LAN interface.
- (e) IDA-based data acquisition front-end hardware with eighteen input channels.

The test grid consists of twenty six locations on the main legs of the tower as shown in (Table 1). Ten reference accelerometers and eight roving accelerometers were used to measure 26 DOF at the test points. Horizontal acceleration was recorded in orthogonal axes (X-axis and Y-axis) at the main legs of the tower as shown in (Table 1) and Fig. 3 shows the direction of measurements on different levels. Two data setups were executed to identify the

natural frequencies of the tower under the effect of the surrounding wind and ambient conditions. In all cases, the sampling frequency on site was 512 Hz and total duration of 300 s was selected for each setup.

Signal processing

The signal data were recorded using PULSE labshop [19] afterwards the signal processing was carried using ARTeMIS extractor [20]. The spectral density matrices

Table 2 Modal results identified using EFDD and SSI

| Mode No | Description | Frequency identified using EFDD (Hz) | Damping ratio EFDD (%) | Frequency identified using SSI-CVA (Hz) | Damping ratio SSI-CVA (%) | MAC |
|---------|----------------------|--------------------------------------|------------------------|---|---------------------------|--------|
| 1 | First Bending (Y–Y) | 0.5704 | 0.7430 | 0.5749 | 1.253 | 0.9951 |
| 2 | Second Bending (Y–Y) | 1.884 | 0.4943 | 1.9239 | 0.3906 | 0.8788 |
| 3 | Third Bending (X–X) | 4.068 | 0.2308 | 4.0676 | 0.3488 | 0.9532 |
| 4 | Fourth Bending (X–X) | 7.567 | 0.1477 | 7.9889 | 0.8862 | 0.9224 |
| 5 | Higher Torsion | 10.1231 | 0.1654 | 10.1856 | 0.9952 | 0.9401 |
| 6 | Higher Torsion | 14.7127 | 0.1430 | 13.8631 | 1.442 | 0.6392 |

are evaluated at discrete equally spaced frequency lines in the range between zero (DC) frequency and Nyquist frequency. This is considered a radix-2 number because of the use of Fast Fourier Transform (FFT). The Hanning window function is the window which is used by default. Also, the overlap between two data segments is taken 66.67%. Moreover, the overlap that is presented in order to reimburse the information loss due to tapering of the data segments that happens due to the data segments being multiplied by the window function. In the case of the self-support tower, the frequency lines were 2048 in order to have enough averages to minimize the noise on the estimated spectral densities. The frequency resolution used 0.01 Hz. The frequency resolution was expected to be sufficient to resolve any closely detected natural frequencies. Also, the used signal processing algorithms are explained as follows [9]:

Fast Fourier transform (FFT)

The fast Fourier transform (FFT) is a quick (computationally efficient) method to calculate the discrete Fourier transform (DFT), The DFT of a discrete-time signal $x(nT)$ is

$$X[k] = \sum_{n=0}^{N-1} X[n] \exp\left(-\frac{i2\pi kn}{N}\right) = \sum_{n=0}^{N-1} X[n] W\left(\frac{nk}{N}\right) \tag{1}$$

where the sampling period T is insinuated in $X[n]$, $X[k]$ is the k th harmonic ($k=0\dots N-1$), $x[n]$ is the n th input sample ($n=0\dots N-1$) Also, N is the frame length, and WN is shorthand for $\exp(-i2\pi/N)$. For a radix-2 FFT, N must be a power or base of 2 [21].

Cross power spectrum

The fast Fourier transform (FFT) is a quick (computationally efficient) way to calculate the discrete Fourier transform (DFT), The DFT of a discrete-time signal $x(nT)$ is.

Cross-power spectrum between two signals $y(t)$ and $x(t)$, it is the product of the Fourier transform of the first signal with the complex conjugate of the Fourier transform of the second signal:

$$G_{yx}(f) = Y(f) X^*(f) \tag{2}$$

where both $Y(f)$ and $X(f)$ are Fourier transforms obtained from the functions $y(t)$ and $x(t)$, and $*$ denotes the complex conjugation.

Auto power spectrum

Auto power spectrum is a spectrum obtained by multiplying $X(f)$ by its own conjugate $X^*(f)$. $G_{xx}(f)$ is real and positive at all frequencies.

Coherence

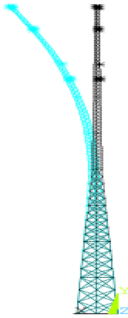
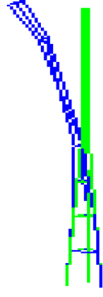

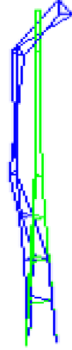
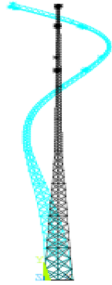



Auto power spectrum is a spectrum obtained by multiplying $X(f)$ by its own conjugate $X^*(f)$. $G_{xx}(f)$ is real and positive at all frequencies.

It is computed as the ratio of the magnitude squared of the cross power spectrum divided by the product of the input and output auto power spectrums as follows:

$$\gamma^2(w) = \frac{|G_{xy}(f)|^2}{|G_{xx}(f) G_{yy}(f)|} \tag{3}$$

The coherence function is real valued having values between zero and one. For output only measurements, coherence function is a very important function because it is expected that the coherence would take high values at resonance frequencies, as a strong vibration pattern exist and a high signal to noise ratio is found.

Table 3 Comparison between identified bending mode shapes using ANSYS FEM and experimental

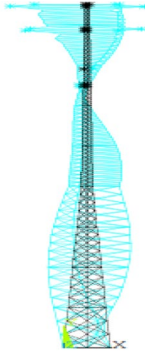

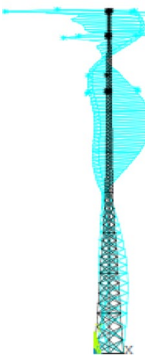

| ANSYS | ARTeMIS |
|---|---|
|  <p>Natural Frequency = 0.5698 Hz</p> |  <p>Natural Frequency = 0.5704 Hz</p> |
|  <p>Natural Frequency = 1.854 Hz</p> |  <p>Natural Frequency = 1.884 Hz</p> |
|  <p>Natural Frequency = 3.547 Hz</p> |  <p>Natural Frequency = 4.068 Hz</p> |
|  <p>Natural Frequency = 6.119 Hz</p> |  <p>Natural Frequency = 7.567 Hz</p> |

Identification of modal properties

The measurement data were recorded in the range of 0–512 Hz. However, only the frequency band from 0 to 20.50 Hz was studied in this analysis. Typical coherence

functions between spectra at the levels of 42.70 and 48.80 m for X and Y directions as shown in Fig. 4. Good correlation is revealed between spectra at this specified range. The resonant peaks of the spectra in the lower frequency range represent the global modes of the whole tower, which are of

Table 3 (continued)

| ANSYS | ARTeMIS |
|--|---|
|  <p data-bbox="592 554 855 579">Natural Frequency = 10.927 Hz</p> |  <p data-bbox="1067 554 1340 579">Natural Frequency = 10.1231 Hz</p> |
|  <p data-bbox="592 949 855 974">Natural Frequency = 14.346 Hz</p> |  <p data-bbox="1067 949 1340 974">Natural Frequency = 14.7127 Hz</p> |

main concern for the purpose of the model calibration. The identification of natural frequency was performed using peak picking method. It is based on the fact that the frequency response function goes through an extreme value around the natural frequency. In the context of output- only response vibration measurements, the frequency response function is replaced by the auto spectra and cross spectra of the output-only data [22]. The method leads to reliable estimates provided that the basic assumptions of low damping and well separated modes are satisfied.

Inspection of all average spectral estimates of ASD and CSD allowed to identify the values of natural frequencies successfully as shown in Fig. 4. The spectra of acceleration in the X & Y directions showed the resonant frequencies (spectral peaks) at 0.5704, 1.884, 4.068 and 7.567 Hz. Beside identified torsion modes at 10.1231 and 14.7127 Hz. Both of the EFDD and SSI techniques were used, both of them produced very close results for the modal frequencies analyzed from 0 to 20.50 Hz as shown in Tables 2 and 3.

Finite element model validation and seismic analysis

In order to verify the FE model, a 3D model was developed using the finite element software ANSYS. The model was updated using experimental modal results obtained by

ARTeMIS extractor software. In order to form a 3D finite element model (FEM), the geometry of the tower was measured in site using a total station instrument. Moreover, for the material characteristics of all steel members a Young’s modulus of 200 GPa, a Poisson’s ratio of 0.3, and steel density of 7850 kg/m³. In addition to, the three legs of the tower are assumed to be restrained at the foundation level. In order to model the three main legs (vertical elements of the tower) BEAM4 element was chosen as well as the corresponding cross section (as described in Clause 2). As for the braces LINK8 element was chosen for its characteristics of carrying axial force both of tension and compression forces, their corresponding cross sections were represented in the model (as described in Clause 2). The dishes and antennas were represented as MASS21 and applied at their corresponding locations. The modal analysis of the updated FEM predicted the dynamic identity of the studied tower in terms of its modal frequencies and corresponding mode shapes. A comparison between the results of the FEM and the experimental results is shown in Table 3 and the comparison shows a good agreement between both results.

There is a crucial importance of maintaining the telecommunication services during the hazards. Due to seismic nature and activities by the red sea coast, structural performance of the existing towers is significant especially for the

Table 4 Identified displacement and axial stresses for different earthquakes

| EQ | Displacement (m) | Axial Stresses (t/m^2) |
|--------------------|------------------|----------------------------|
| 1995 Gulf of Aqaba | | |
| | | |
| 1995 Kobe, Japan | | |

top part of the tower, where the antennas are attached. In order to study the seismic effect on the tower. Three generated seismic events were used 1995 Gulf of Aqaba, 1940 Imperial Valley and 1995 Kobe, Japan earthquakes time history records were applied to the model individually using time history analysis, the events were of magnitude $M_w = 7.1$ [23], 6.95 and 6.90 [24], respectively, and maximum acceleration during each event 0.896, 2.755 and 2.705 m/sec^2 , respectively. Generation of earthquakes been developed and applied as per [13]. Antenna supporting towers should comply with strict serviceability criteria. Seismic amplification may affect the top part of the tower where the antennas are attached and it should not result in any local permanent deformation after the earthquake.

The results of the maximum displacement at the top of the tower obtained from seismic loading due to the earthquakes are 0.091, 0.2964 and 0.3637 m, respectively. Also, the axial stresses obtained from the earthquakes are 0.0509, 0.2036 and 0.1918 t/cm^2 , respectively. Table 4 shows for each case displacement vs time and the axial stresses vs time.

Maximum displacement allowable as per Table (9.1), ECP-205 [25] is 0.1 m and the maximum axial compression stresses allowable as per ECP-205 is 0.9840 t/cm^2 for the mast's vertical legs of steel pipe section 75 × 5.5 mm. Therefore, the tower falls in the allowable limits for the axial stresses under the acting loads, while exceeding the allowable limits for displacement in case of 1940 Imperial Valley and 1995 Kobe, Japan earthquakes.

Conclusions

The paper presents an experimental and analytical dynamic study of an existing telecommunication tower using ambient vibrations. Being a very flexible steel structure, setting up the test grid and mounting the sensors along the height of the tower was a real challenge. To reach the test grid points of the tower very skillful trained engineer climbed the tower to gain access to different levels along the height of the tower while the tower was swinging. This reflects how

valuable are the results of AVT as very few studies illustrate such complicated experimental work. Both of the EFDD and SSI techniques were utilized to perform experimental modal analysis. The experimental modal analysis was successful in identifying the natural frequencies and their corresponding mode shapes in the range 0–20.50 Hz. The dynamic modal behavior of the tower included bending and torsion modes.

The FE model in ANSYS was thoroughly updated to match the identified modal properties. 7 global modes were selected to tune with the results of experimental modal analysis. Good correlation between experimental and theoretical model enabled the updated model to provide reliable predictions to evaluate the structural performance of the tower under seismic loading. The accurate data concerning the geometrical, material properties, connections details and boundary conditions are essential to build an updated base line model representing the real dynamic behavior.

The seismic analysis of the tower under three selected seismic events was applied using time history analysis. The structural performance of the tower was predicted showing no strength deficiency under load patterns. In case of 1995 Gulf of Aqaba earthquake there is no influence on the structural integrity of the tower or the antenna serviceability criteria due to the motion of the top part of the tower, however in the case of 1940 Imperial Valley and 1995 Kobe, Japan earthquakes the maximum limit to displacement is exceeded and would require strengthening for the tower for such case in order to comply with the code limits. Accordingly the adopted plan in this study shown to be accurate and valid to assess the structural performance of lattice self-supporting towers under different structural loadings. The updated FE model can be extensively useful if the tower need to be investigated for adding larger or additional antenna and also for any future structural modifications.

Funding No funding was received for conducting this study.

Declarations

Conflict of interest The authors have no financial or proprietary interests in any material discussed in this article. On behalf of all authors, the corresponding author states that there is no conflict of interest.

References

1. Wahba YMF, Madugula MKS, Monforton GR (1998) Dynamic response of guyed masts. *Eng Struct* 20(12):1097–1011
2. Wahba YMF, Madugula MKS, Monforton GR (1998) Effect of icing on the free vibration of guyed antenna towers. *Atmos Res* 46:27–35
3. Wahba YMF, Madugula MKS, Monforton GR (1998) Evaluation of non-linear analysis of guyed antenna towers. *Comput Struct* 68:207–212
4. Abdel-Ghaffer AM, Scanlan RH (1985) Ambient vibration studies of Golden Gate Bridge. I: suspended structure. *J Eng Mech* 111(4):463–482
5. Okauchi I, Miyata T, Tatsumi M, Sasaki N (1997) Field vibration test of a long span cable-stayed bridge using large exciters. *J Struct Eng Earthq Eng* 14(1):83–93
6. Chuna A, Caetano E, Delgado R (2001) Dynamic test on large cable-stayed bridge. *J Bridge Eng* 6(1):54–62
7. Ren WX, Zhao T, Harik IE (2004) Experimental and analytical modal analysis of a steel arch bridge. *J Struct Eng* 130(7):1022–1031
8. Brownjohn JMW (2003) Ambient vibration studies for system identification of tall buildings. *J Earthq Eng Struct Dyn* 32:71–75
9. Saudi G (2014) Structural assessment of a guyed mast through measurement of natural frequencies. *Eng Struct* 59:104–112
10. Saudi G and Kamal H (2014) Ambient vibration testing of full-scale wind turbine tower. In: Tenth international conference on the role of engineering towards a better environment, 15–17 December, Alexandria, Egypt
11. Luis Garcia K, Maes K, Elena Parnas V, Lombaert G (2020) Operational modal analysis of a self-supporting antenna mast. *J Wind Eng Ind Aerodyn* 209(2021):104490
12. Capilla JAJ, Slu-Kul Au, BrownJohn JMW (2021) Emma Hudson (2021) Ambient vibration testing and operational modal analysis of monopole telecoms structure. *J Civ Struct Health Monitor* 11:1077–1091
13. Saudi GNE, Aly EHAH (2017) Structural response of a self-supporting tower under seismic loads, Al-Azhar University Civil Engineering Research Magazine (CERM), Vol. (39), No. (1)
14. International Journal of Engineering: Ghodrati Amiri G, Massah SR and Boostan A (2007) Seismic response of 4-legged self-supporting telecommunication towers. *Transactions B* 20(2):107–125
15. Jaishi B, Ren WX, Zong ZH, Maskey PN (2003) Dynamic and seismic performance of old multi-tiered temples in Nepal. *J Eng Struct* 25(14):1827–1839
16. Dyck C, Ventura CE (2000) Ambient vibration measurement of heritage court tower. IMAC 18: Proceedings of the international modal analysis conference (IMAC), San Antonio, Texas, USA, February 7–10
17. Kyung-Won M, Junhee K, Sung-Ah P, Chan-Soo P (2010) Ambient vibration testing for story stiffness estimation of a heritage timber building. *The Sci World J* 2013(9):198483
18. Endrun B, Ohrnberger M, Savvaidis A (2010) On the repeatability and consistency of three-component ambient vibration array measurements. *Bull Earthq Eng* 8(3):535–570
19. PULSE (2006) Labshop, Version 11.2.2. Brüel & Kjær Sound and Vibration Measurements A/S
20. Structural Vibration Solutions ApS (2019) ARTeMIS Extractor, User's Manual, Denmark
21. Chasseing R (2005) Digital signal processing and applications with the C6713 and C6416 DSK. John Wiley and Sons
22. Bendat JS, Piersol AG (1993) Engineering applications of correlation and spectral analysis. John Wiley and Sons
23. Al-Tarazi E (2000) The Major Gulf of the Aqaba earthquake, 22 November 1995 – maximum intensity distribution. *Nat Hazards* 22:17–27
24. Pacific Earthquake Engineering Research Center (PEER) (2022), <https://ngawest2.berkeley.edu>, 1 Nov 2022
25. Egyptian Code of Practice for Steel Construction and Bridges, Number 205 (2012), pp 132

Springer Nature or its licensor (e.g. a society or other partner) holds exclusive rights to this article under a publishing agreement with the author(s) or other rightsholder(s); author self-archiving of the accepted manuscript version of this article is solely governed by the terms of such publishing agreement and applicable law.